Demonstration of high-gradient electron acceleration driven by subnanosecond pulses of Ka-band superradiance

N. S. Ginzburg,[1] A. E. Fedotov,[1] S. V. Kuzikov,[2] K. A. Sharypov,[3] V. G. Shpak,[3] S. A. Shunailov,[3] A. A. Vikharev,[1,3] M. I. Yalandin,[3] and I. V. Zotova[1,3]

[1]*Institute of Applied Physics RAS, 603950, Nizhny Novgorod, Russia*
[2]*Euclid Techlabs LLC, Bolingbrook, Illinois 60440, USA*
[3]*Institute of Electrophysics UB RAS, 620016, Yekaterinburg, Russia*

(Received 31 January 2023; accepted 4 May 2023; published 7 June 2023)

We report the high-gradient acceleration of electrons driven by a subnanosecond pulse of Ka-band Cherenkov superradiance (SR). The experiments are carried out in a combined "generator-accelerator" scheme, powered by two electron beams from a coaxial explosive-emission graphite cathode. The outer tubular beam (≈300 keV; ≈2.3 kA) propagates along the periodic slow-wave structure (SWS) and generates a backward moving gigawatt-level SR pulse, which pumps a low-Q "pill-box" resonator located at the SWS input. The inner paraxial test beam (≈250 keV; ≈150 A) passes through a hole in the resonator wall and is accelerated in extreme SR fields exceeding 500 MV/m. The energy of accelerated electrons is estimated by measuring the test beam current after it passes through aluminum filters (foils) that absorb low-energy electrons. It is shown that the test beam contains fractions with a maximum energy of 1.25 MeV, which, taking into account the pill-box length of 4 mm, corresponds to the extremely high averaged accelerating gradient of 250 MV/m.

DOI: 10.1103/PhysRevAccelBeams.26.060401

Along with other parameters, the most important characteristic of charged particle accelerators is the accelerating gradient, which, in the case of powering electrodynamic structures with long-wavelength (X and S band) klystrons, is typically significantly lower than 100 MV/m [1,2]. Currently, the problem of overcoming the specified level has stimulated the development of brand-new physical concepts, such as laser-plasma and beam-plasma acceleration [3–8] together with acceleration based on optics-to-terahertz radiation conversion [9–11]. Nevertheless, high-gradient electron acceleration (HGEA) in "warm" metal structures remains relevant, which is associated with an increase in the power of radiation sources in the centimeter, millimeter, and submillimeter wave bands [12–16].

Besides, the solution of the radio-frequency (rf) breakdown and structure degradation problems is facilitated by using the short-action (pulsed) radiation with nanosecond duration. This, in particular, stimulates research on the implementation of laser-controlled semiconductor switches for the formation of nanosecond pulses from the radiation of a microsecond megawatt gyrotron [17,18]. Based on this approach, electric fields of 200–230 MV/m have been reached in breakdown tests of accelerating structures. The highest accelerating fields (up to 300–400 MV/m) in short pulses are declared when using wakefield radiation [19,20] from preformed ultrarelativistic electron bunches with a length smaller than the wavelength.

In order to direct generate extremely high-power nanosecond and subnanosecond pulses for HGEA, we suggest the alternative method which is based on Cherenkov superradiance (SR) of extended (in the scale of the radiation wavelength) electron bunches [21–25] interacting with a backward-wave in a periodical slow-wave structure (SWS). In this case, coherent pulse emission occurs due to the development of longitudinal microbunching and slippage of the backward wave with respect to the electron bunch, which is, similarly to SR in optics [26,27], should be shorter than the so-called cooperative length. By analogy with the interaction in backward-wave oscillators (BWOs), such a specific mechanism of short pulse emission is referred to as SR BWOs. However, unlike the BWOs, the peak power of the SR pulse, which accumulates the energy of successive electron fractions, can exceed the power of the electron beam [21].

To date, in the Ka band, compact (table-top) SR BWOs, powered by 200–300 keV electron beams, provide record-breaking radiation power up to 2 GW with a pulse full duration of 0.3 ns [21,22]. SR pulses can have a stable generation phase which can be controlled by an external seed rf signal [23]. Viability for the advancement of SR generators with oversized electrodynamic structures into

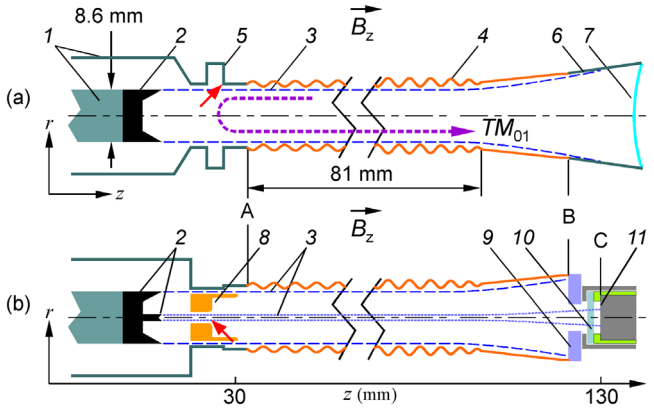

FIG. 1. (a) Original scheme of the 1-GW Ka-band SR BWO with one tubular high-current electron beam. (b) The experimental HGEA scheme with two coaxial beams. The numbers indicate the following: 1—coaxial feeder; 2—graphite cathode(s); 3—electron beam(s); 4—SWS; 5—resonant reflector; 6—radiating horn; 7—vacuum window; 8—"pill-box" resonator; 9—metallic diaphragm; 10—aluminum filter; and 11—current sensor for diagnostics of the paraxial beam.

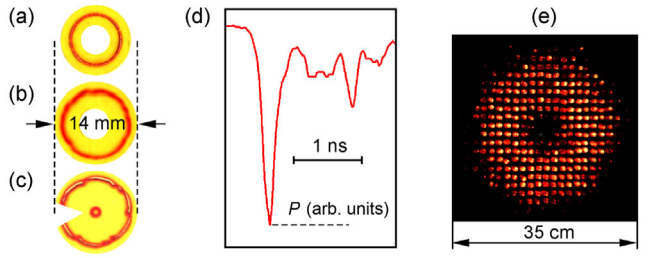

FIG. 2. (a) and (b) Reprints of the electron beam powering the original configuration of the SR BWO [Fig. 1(a)], in cross sections A and B, respectively. (c) Reprints of the coaxial beams of the experimental HGEA scheme [Fig. 1(b)], in the cross section B. (d) Detected 1-GW Ka-band SR pulse in the power-time coordinates (P, t). (e) Gas-discharge panel luminescence under the action of a single SR pulse.

the short-wavelength part of the millimeter band was also demonstrated with a power level of up to 70 MW in G band [24] and over 100 MW in W band [25]. Listed unique radiation parameters make SR generators rather attractive for accelerator applications.

In this paper, we report the acceleration of electrons with a gradient well above 100 MV/m using the 38-GHz 1-GW SR BWO [21] equipped with a single-cell resonant accelerating structure. Despite the presence of extreme rf fields, high values of the accelerating gradient are reached in the SR pulse since the subnanosecond duration prevents the development of breakdown.

The original scheme of the SR BWO, which is used in the HGEA experiments, is shown in Fig. 1(a). The tube is powered by a tubular electron beam with a current of 2.3 kA. The beam is kept thin [Figs. 2(a) and 2(b)] during its transportation along the SWS due to the strong axial magnetic field $B_z \approx 6.5$ T created by a pulsed solenoid. Note that, in contrast to [21], the injector voltage pulse, formed by the pulsed power supply system [28], was elongated twice to ≈2 ns; thus, the beam length exceeds the cooperative length. As a result, a stable subnanosecond SR peak with a power of ≈1 GW (measured by a detector and a calorimeter) is followed by a series of chaotic peaks with a power of 100–300 MW [Fig. 2(d)], which is typical for SR BWOs with elongated beams. According to simulations based on the KARAT code [29], at 1-GW SR power, the maximum strength of the radial and axial components of the electric field, which are approximately equal in the point at the reflector edge [indicated by an arrow in Fig. 1(a)], is at least 230 MV/m. Nevertheless, the presence of additional peaks [Fig. 2(d)], as well as a shot-to-shot stable image of the wave beam [Fig. 2(e)], show the absence of the development of rf breakdowns in the specified fields, the maximum value of which was reached in about 300 ps. This allowed us to expect that the accelerating structure would withstand rf fields sufficient for the HGEA for fractions of a nanosecond.

For the HGEA experiments, it was supposed to concentrate rf fields in a half-wave "pill-box" resonator [Fig. 3(a)]. The resonator has a low Q factor, which ensured its pumping with a subnanosecond SR pulse. The structure of the field in the resonator at the maximum pumping is shown in [Fig. 3(b)]. According to the simulation, at 1-GW peak power of the SR pulse [Fig. 2(d)], the accelerating field on the pill-box axis reaches about of 800 MV/m, while the electric field at the resonator wall is about of 1 GV/m.

For the presented experiments, the combined "generator-accelerator" scheme was developed [30], in which the "pill-box" resonator is incorporated into the vacuum volume of the SR BWO before the slow-wave structure [Fig. 1(b)]. This scheme utilizes two electron beams which are formed by the coaxial explosive emission graphite cathodes powered by a single (≈ −300 kV/≈ 2 ns) voltage pulse. The outer 300 keV/2.3 kA tubular beam feeds the slow-wave structure and generates the backward moving SR pulse. The second paraxial beam with a diameter of 1 mm and a slightly lower (due to the beam potential depression)

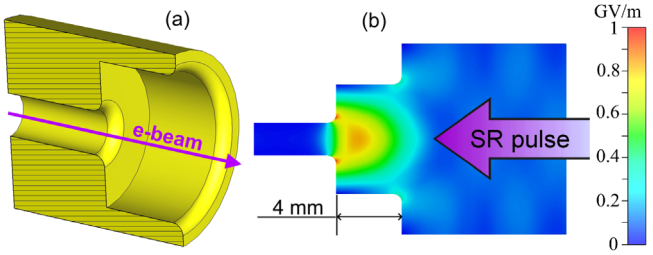

FIG. 3. (a) 3D view of the semiopen "pill-box" resonator. (b) E_z—field distribution at the moment of maximum resonator pumping, found in simulation with 1-GW SR pulse from Fig. 2(d).

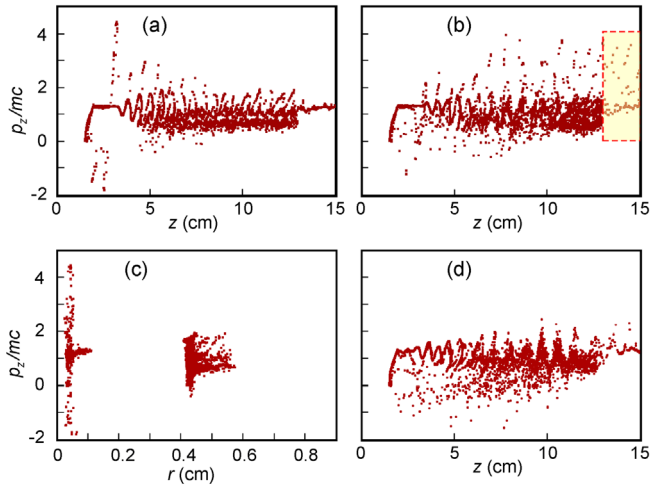

FIG. 4. Phase portraits of the beams: on the plane $(p_z/mc, z)$ at the time of 1.03 ns (a) and 1.37 ns (b) from the start of the cathodes' emission; on the plane $(p_z/mc, r)$ at the time of 1.03 ns (c); on the plane $(p_z/mc, z)$ at the time of 1.37 ns for the BWO SR scheme without the accelerator unit [Fig. 1(a)], supplemented with a paraxial beam (d).

energy of ≈250 keV, confirmed by measurements (see below), is formed by the central sharp-edge core of the cathode. This test beam passes through the "pill-box" hole and is accelerated after the resonator is pumped with the SR pulse. The pill-box resonator is fixed on steel foil lamellas [31], which, however, do not prevent the outer beam from passing through a 0.5-mm concentric slot between the resonator and the moderately oversized SWS input [see beam imprints in Fig. 2(c)]. Note also, that the paraxial beam has a current of ≈150 A, which is much less than the current of the external beam and does not affect the SR generation.

When preparing the experiments, the combined scheme was simulated [30] in the configuration presented in Fig. 1(b). Figure 4 shows the phase portraits of electrons in planes p_z/mc, z and p_z/mc, r (where p_z is the axial momentum). The distribution in Fig. 4(a) is obtained in the plane p_z/mc, z at the moment $t = 1.03$ ns when the axial electric rf field at the "pill-box" input [marked by an arrow in Fig. 1(b)] reaches a maximum of ≈400 MV/m. Taking into account the well-known relation between the axial momentum of a relativistic electron and its kinetic energy ε_k

$$(\varepsilon_k + mc^2)^2 = (p_z c)^2 + (mc^2)^2, \qquad (1)$$

for the maximum $p_z/mc \approx 4.4$, we obtain $\varepsilon_k \approx 1.8$ MeV. Thus, the increase in ε_k from the initial 250 keV is 1.55 MeV, which, with the "pill-box" length of 4 mm, means that the average accelerating gradient reaches ≈390 MV/m. The phase portrait on plane p_z/mc, r [Fig. 4(c)] obtained at the same time as Fig. 4(a), demonstrates that the most accelerated electrons belong to the paraxial beam.

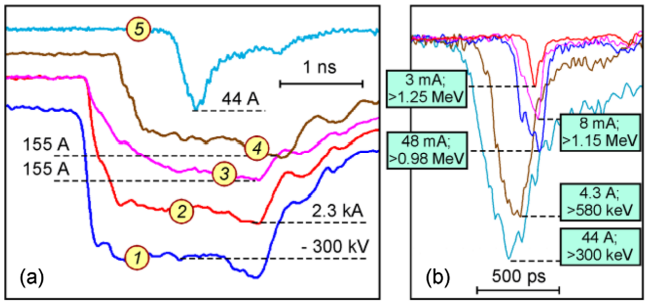

FIG. 5. (a) Waveforms of the cathode voltage pulse (1) and the beam current pulses: (2) external generating beam; (3,4) paraxial test beam at input and output of the SWS, respectively; and (5) fraction of the paraxial beam accelerated above 300 keV. All pulses are synchronized in time. (b) Current pulses from the fast-response sensor behind Al filters with a cutoff energy of up to 1.25 MeV.

At $\varepsilon_k \approx 1.8$ MeV, the electron velocity is $\approx 0.96c$; thus, at the time $t = 1.37$ ns, the accelerated electron fraction will be in cross sections $z > 13$ cm [shaded area in Fig. 4(b)], which corresponds to the position of the collector current sensor in the experiment [section "C" in Fig. 1(b)]. In accordance with the phase portrait presented in Fig. 4(b), the maximum p_z/mc in this zone reaches ≈3.6, which corresponds to $\varepsilon_k \approx 1.4$ MeV. Such a decrease in energy, probably, is caused by the nonsynchronous interaction of electrons with the fields of the SR pulse reflected from the resonator after its pumping [30], when the particles overtake the wave on the way to the sensor. Note also that the acceleration effect disappears [Fig. 4(d)] when the pill-box resonator is removed from the scheme despite the fact that the copropagating SR pulse in the original scheme [Fig. 1(a)] has a larger amplitude and shorter duration than in the case of reflection from the pill-box resonator [Fig. 1(b)].

Experimental conditions were consistent with the numerical model of HGEA. The SR pulse shown in Fig. 2(d) is recorded by the detector. The total beams currents [curves (2), (3), and (4) in Fig. 5(a)] are registered by the collector sensor with a resolution of ≈0.1 ns, and their emission onset is determined by the method [31], which also provides the restoration of the voltage pulse shape and amplitude at the cathode (*ibid.*). The energy of accelerated electrons is estimated based on measurements of the test beam current after its propagation through a system of aluminum foils (Al filters) with known cutoff energies [32]. Note, that the used registration technique is a qualitative method that shows the existence of electrons with energy higher than some limit but does not show the exact number of such electrons.

The energy of the test paraxial beam [curve (3) in Fig. 5(a)] measured in the absence of SR generation (the external beam is blocked) is ≈250 keV since the beam does not pass through a 320-μm Al filter. When the SR pulse is generated, the "pill-box" resonator is pumped and the test

beam is accelerated. As a result, when the test beam passes to the collector through a 400-μm filter, the current of electrons with energies >300 keV is recorded [curve (5) in Fig. 5(a)].

A more accurate measurement of the energy of accelerated electrons is carried out using the fast sensor [33] possessing a response of 14 V per 1-A bunch current. Its time resolution of ≈10 ps was determined by the drain time of absorbed charge from the collector representing the end face of the coaxial line with a multistep junction (6.17–50 Ω) to the oscilloscope cable. Collector and shielding thin foil performed a miniature radial transmitting line matched with coaxial one. We note that the limited bandwidth (33 GHz) of the oscilloscope used did not allow us to see the time-discriminated current bursts from individual accelerated bunches [31]. According to the imprint of the paraxial test beam [Fig. 2(c)], the sensor with a collector diameter of 6 mm registered the entire current passed through the filters. A set of registered current pulses at different cutoff energies is shown in Fig. 5(b) demonstrating the presence of the accelerated electron fraction with an energy surpassing the cutoff ≈1.25 MeV of the 2.65-mm thick Al filter. Note that in the absence of the pill-box resonator, the test electron beam did not pass through a filter 400 μm thick with a cutoff energy of ≈300 keV.

As follows in Fig. 5(b), the current pulses of higher-energy electron fractions are shortened and "embedded" into the envelopes of the current pulses, which include less energetic particles. At $\varepsilon_k \geq 1.25$ MeV, the duration of the current pulse is not more than the sum of (3–4) periods of the accelerating rf field and a measured charge is ≈0.2 pC. The current pulse of particles with $\varepsilon_k \geq 300$ keV has a much longer duration at a full measured charge of ≈25 nC. With an increase in the Al-filter cutoff energy, the leading edges of the current pulses appear later in accordance with the rise of the rf field during the resonator pumping. Such a delay was independent of vacuum in the range of 10^{-2}–10^{-4} torr.

Since the simulation revealed a difference in the energy maxima (1.8 and 1.4 MeV) in sections A and C [Figs. 4(a) and 4(b)], it can be assumed that in the experiment the maximum energy of electrons behind the resonator was hundreds of kilo electronvolts higher than that measured by the collector sensor after the filter at the SWS output. Thus, the obtained value $\varepsilon_k \approx 1.25$ MeV is a lower estimate. When averaged over the pill-box length of 4 mm, this energy gain corresponds to the high acceleration gradient of about 250 MV/m.

In conclusion, we have demonstrated for the first time the Ka-band HGEA in a resonant metal structure with an accelerating gradient exceeding several times the values obtained on the basis of long-wavelength klystrons. High gradients are reached due to short exposure times in subnanosecond SR pulses; so no additional shortening of the pulse is required compared, for example, with gyrotron experiments [17,18]. In addition, the total increase in the electron energy above 1 MeV is higher than the values obtained in acceleration on the basis of optics-to-terahertz conversion [9–11]. The demonstrated results are an important step in the development of compact and more affordable accelerator facilities. A more practical configuration would be to extract a GW superradian pulse from the generator to power a separate accelerating structure. For example, simulations show [34] that a traveling-wave accelerating structure powered by the same SR pulse allows achieving the energy gain of over 7 MeV. Besides, several phase-controlled SR generators [23] can be used to power a sequence of accelerating structures.

The work was supported by the Russian Science Foundation under Project 21-19-00260. The pulsed power equipment belonging to the Collective Use Center of the Institute of Electrophysics UB RAS and earlier developed under the Program No. 122011200367-7 was used in the experiments. The authors note the contribution of the Ural Federal University, which provided the Tektronix DPO73304D oscilloscope for measurements.

[1] S. Doebert *et al.* (CLIC/CTF3 Collaboration), Status and future prospects of CLIC, in *Proceedings of the XXIV Linear Accelerator Conference, LINAC-2008, Victoria, BC, Canada* (TRIUMF, Vancouver, Canada, 2008).

[2] Xiaoxia Huang, Wencheng Fang, Qiang Gu, and Zhentang Zhao, Nucl. Instrum. Methods Phys. Res., Sect. A **854**, 45 (2017).

[3] A. J. Gonsalves, K. Nakamura, J. Daniels, C. Benedetti, C. Pieronek, T. C. H. de Raadt, S. Steinke, J. H. Bin, S. S. Bulanov, J. van Tilborg *et al.*, Phys. Rev. Lett. **122**, 084801 (2019).

[4] J. P. Palastro, J. L. Shaw, P. Franke, D. Ramsey, T. T. Simpson, and D. H. Froula, Phys. Rev. Lett. **124**, 134802 (2020).

[5] O. Jakobsson, S. M. Hooker, and R. Walczak, Phys. Rev. Lett. **127**, 184801 (2021).

[6] K. V. Lotov, Phys. Plasmas **24**, 023119 (2017).

[7] M. Turner *et al.* (AWAKE Collaboration), Phys. Rev. Lett. **122**, 054801 (2019).

[8] E. Adli *et al.* (AWAKE Collaboration), Nature (London) **561**, 363 (2018).

[9] D. Zhang, A. Fallahi, M. Hemmer, X. Wu, M. Fakhari, Y. Hua, H. Cankaya, A.-L. Calendron, L. E. Zapata, N. H. Matlis, and F. X. Kärtner, Nat. Photonics **12**, 336 (2018).

[10] M. T. Hibberd, A. L. Healy, D. S. Lake, V. Georgiadis, E. J. H. Smith, O. J. Finlay, T. H. Pacey, J. K. Jones, Y. Saveliev, D. A. Walsh, E. W. Snedden, R. B. Appleby, G. Burt, D. M. Graham, and S. P. Jamison, Nat. Photonics **14**, 755 (2020).

[11] H. Tang, L. Zhao, P. Zhu, X. Zou, J. Qi, Y. Cheng, J. Qiu, X. Hu, W. Song, D. Xiang, and J. Zhang, Phys. Rev. Lett. **127**, 074801 (2021).

[12] Y. Cao, J. Sun, Z. Fan, Z. Song, G. Zhang, N. Tan, P Wu, and M. Zhu, IEEE Electron Device Lett. **40**, 1530 (2019).

[13] V. V. Rostov, R. V. Tsygankov, P. V. Vykhodsev, V. Y. Konev, and A. S. Stepchenko, IEEE Electron Device Lett. **42**, 935 (2021).
[14] L. J. R. Nix, L. Zhang, W. He, C. R. Donaldson, K. Ronald, A. W. Cross, and C. G. Whyte, Phys. Plasmas **27**, 053101 (2020).
[15] W. Lawson, J. P. Calame, G. S. Nusinovich, and B. Hogan, THz Sci. Technol. **10**, 1 (2017).
[16] J. L. Hirshfield, E. V. Kozyrev, M. A. LaPointe, O. A. Nezhevenko, S. V. Shchelkunov, and V. P. Yakovlev, AIP Conf. Proc. **877**, 280 (2006).
[17] S. V. Kutsaev, B. Jacobson, A. Yu. Smirnov, T. Campese, V. A. Dolgashev, and V. Gonch, Phys. Rev. Appl. **11**, 034052 (2019).
[18] M. A. K. Othman, J. Picard, S. Schaub, V. A. Dolgashev, S. M. Lewis, J. Neilson, A. Haase, S. Jawla, B. Spataro, R. J. Temkin *et al.*, Appl. Phys. Lett. **117**, 073502 (2020).
[19] M. D. Forno, V. Dolgashev, G. Bowden, C. Clarke, M. Hogan, D. McCormick, A. Novokhatski, B. O'Shea, B. Spataro, S. Weathersby, and S. G. Tantawi, Phys. Rev. Accel. Beams **19**, 011301 (2016).
[20] W. H. Tan, S. Antipov, D. S. Doran, G. Ha, C. Jing, E. Knight, S. Kuzikov, W. Liu, X. Lu, P. Piot, J. G. Power, J. Shao, C. Whiteford, and E. E. Wisniewski, Phys. Rev. Accel. Beams **25**, 083402 (2022).
[21] A S. D. Korovin, A. A. Eltchaninov, V. V. Rostov, V. G. Shpak, M. I. Yalandin, N. S. Ginzburg, A. S. Sergeev, and I. V. Zotova, Phys. Rev. E **74**, 016501 (2006).
[22] V. V. Rostov, I. V. Romanchenko, M. S. Pedos, S. N. Rukin, K. A. Sharypov, V. G. Shpak, S. A. Shunailov, M. R. Ul'masculov, and M. I. Yalandin, Phys. Plasmas **23**, 093103 (2016).
[23] G. A. Mesyats, N. S. Ginzburg, A. A. Golovanov, G. G. Denisov, I. V. Romanchenko, V. V. Rostov, K. A. Sharypov, V. G. Shpak, S. A. Shunailov, M. R. Ulmaskulov, M. I. Yalandin, and I. V. Zotova, Phys. Rev. Lett. **118**, 264801 (2017).
[24] N. S. Ginzburg, A. M. Malkin, A. S. Sergeev, I. V. Zheleznov, I. V. Zotova, V. Yu. Zaslavsky, G. Sh. Boltachev, K. A. Sharypov, S. A. Shunailov, M. R. Ul'masculov, and M. I. Yalandin, Phys. Rev. Lett. **117**, 204801 (2016).
[25] N. S. Ginzburg, V. Yu. Zaslavsky, A. M. Malkin, A. S. Sergeev, I. V. Zotova, K. A. Sharypov, S. A. Shunailov, V. G. Shpak, M. R. Ul'masculov, and M. I. Yalandin, Appl. Phys. Lett. **117**, 183505 (2020).
[26] N. Scribanowitz, I. P. Hermann, J. C. MacGillivray, and M. S. Feld, Phys. Rev. Lett. **30**, 309 (1973).
[27] R. Bonifacio, B. W. J. McNeil, and P. Pierini, Phys. Rev. A **40**, 4467 (1989).
[28] M. I. Yalandin, S. K. Lyubutin, M. R. Oulmascoulov, S. N. Rukin, V. G. Shpak, S. A. Shunailov, and B. G. Slovikovsky, IEEE Trans. Plasma Sci. **30**, 1700 (2002).
[29] V. P. Tarakanov, *User's Manual for Code KARAT* (Berkeley Research Associates Inc., Springfield, VA, 1992).
[30] N. S. Ginzburg, A. E. Fedotov, S. V. Kuzikov, A. M. Malkin, K. A. Sharypov, S. A. Shunailov, A. A. Vikharev, M. I. Yalandin, and I. V. Zotova, Phys. Plasmas **29**, 123101 (2022).
[31] K. A. Sharypov, M. R. Ul'masculov, V. G. Shpak, S. A. Shunailov, M. I. Yalandin, G. A. Mesyats, V. V. Rostov, and M. D. Kolomiets, Rev. Sci. Instrum. **85**, 125104 (2014).
[32] V. F. Baranov, *Dozimetry of Electron Radiation* (Atomizdat, Moscow, USSR, 1974).
[33] G. A. Mesyats, M. I. Yalandin, N. M. Zubarev, A. G. Sadykova, K. A. Sharypov, V. G. Shpak, S. A. Shunailov, M. R. Ulmaskulov, O. V. Zubareva, A. V. Kozyrev, and N. S. Semeniuk, Appl. Phys. Lett. **116**, 063501 (2020).
[34] Y. Y. Danilov, N. S. Ginzburg, I. V. Zotova, and M. I. Yalandin, Tech. Phys. Lett. **48**, 27 (2022).